Abrasive Wear Performance of Tropical Hardwoods Under Two-Body Contact

Aubin Takoudjou Talla [a,*] René Ngouffo Koukougnang [b,c] Ulrich Gael Azeufack Tonfack,[c] Lie Régis Moumbina,[a] Claude Takoumbe [b] Sandrine Mabekou,[a] and Pierre Kisito Talla [a]

* *Corresponding author: takoudjouaubin@gmail.com, ngouffo2002@yahoo.fr*

DOI: 10.15376/biores.21.4.11211-11227

GRAPHICAL ABSTRACT

Better understanding wood wear behavior for sustainable materials and improved industrial performance.

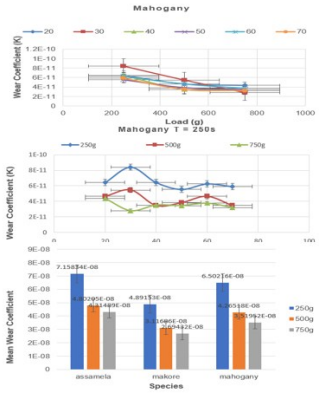


1-Materials





2- Experimental setup



3- Main results

Abrasive Wear Performance of Tropical Hardwoods Under Two-Body Contact

Aubin Takoudjou Talla [a,*] René Ngouffo Koukougnang [b,c] Ulrich Gael Azeufack Tonfack,[c] Lie Régis Moumbina,[a] Claude Takoumbe [b] Sandrine Mabekou,[a] and Pierre Kisito Talla [a]

Abrasive wear behavior was studied for three tropical hardwood species, *Tieghemella heckelii* (makore), *Khaya anthotheca* (mahogany), and *Pericopsis elata* (assamela), under various normal loads and sliding speeds. Two-body abrasion tests were performed perpendicular to the grain, dry and without lubrication, at sliding speeds of 20 to 70 rpm and under normal loads of 250, 500, and 750 g. The wear coefficient (*k*) was determined from the slope of the quasi-linear steady-state portion of the wear volume and sliding distance relationship. All species exhibited an initial running-in phase followed by a steady-state wear regime. Makore displayed the lowest average wear coefficients, while assamela exhibited the highest values. Increasing the load from 250 to 500 g reduced the wear coefficient by 32.9% to 36.3%, while the reduction between 500 and 750 g was more moderate (10.1% to 17.5%), indicating a non-linear load dependence. This behavior could be related to variations in actual contact conditions and deformation of the wood's cellular structure. Sliding speed induced a non-monotonic, species-dependent response, with critical speed ranges corresponding to minimum and maximum wear coefficients. Overall, the results demonstrate that resistance to abrasive wear depends on the combined effects of wood species, normal load, and sliding speed. These results provide useful guidance for selecting tropical hardwoods for applications involving abrasive mechanical contact.

DOI: 10.15376/biores.21.4.11211-11227

Keywords: Wear coefficient; Tropical hardwoods; Sliding abrasion; Sliding speed; Tribological behavior; Surface degradation

Contact information: a: Laboratory of Mechanics and Modeling of Physical Systems (L2MSP), Faculty of Science, University of Dschang, Dschang, West Cameroon; b: Higher Technical Teachers' Training College (HTTTC), Department of Mechanical Engineering, University of Buea, Kumba, Cameroon; c: Department of Mechanical and Industrial Engineering, Faculty of Engineering and Technology, University of Buea, Buea, Cameroun;
** Corresponding author: takoudjouaubin@gmail.com, ngouffo2002@yahoo.fr*

INTRODUCTION

Wood is a renewable material widely used in engineering applications due to its advantageous mechanical properties. However, when exposed to repeated friction or abrasion, its surface can gradually deteriorate, affecting its dimensional stability, appearance, and functional performance. It is therefore important to fully understand wood's resistance to abrasive wear in order to select the appropriate material and predict the durability of wooden components subjected to mechanical contact.

Recent tribological studies have shown that wood wear is not only species-dependent but also strongly influenced by operational parameters such as normal load and sliding speed. For instance, Guan *et al.* (2024) demonstrated that densified wood subjected to different loads and speeds exhibits increasing wear volume, highlighting how sliding speed can significantly alter the dominant abrasion mechanisms at the contact interface. Similarly, Snow *et al.* (2022) confirmed that thermo-mechanical densification significantly enhances abrasion resistance in several US hardwood species, underscoring the role of internal structure in surface durability. Nasir and Cool (2018) also highlighted the influence of fiber orientation and mechanical anisotropy, showing that the direction of loading relative to grain structure modulates wear rates, thereby emphasizing the need to account for both mechanical and structural variables.

In engineered wood systems, surface wear and machining performance are further affected by the interaction between tool geometry and processing conditions. Torkghashghaei *et al.* (2022) demonstrated that optimizing the micro-geometry of carbide-tipped cutting tools using PVD (physical vapor deposit) coatings results in measurable reductions in wear rates during sawmill operations, underscoring the importance of tool–material contact dynamics. Likewise, Gendvilas *et al.* (2024) investigated resistance drilling in hardwoods and revealed that variations in feed rate and spindle rotation significantly influence drilling precision and indirectly reflect the wood's response under frictional stress. In a similar manner, Ghadiri *et al.* (2021) showed that increased cutting speeds during milling of laminated wood composites can induce thermal softening, altering the wear mechanism from abrasive to adhesive and thereby modifying wear behavior.

Recent studies on the thermo-hydro-mechanical (THM) densification of tropical hardwoods have further highlighted the potential for improving wear resistance through structural modification. In Costa Rica, Tenorio and Moya (2020) reported that THM densification of species, such as *Alnus acuminata*, *Vochysia ferruginea*, and *V. guatemalensis*, enhances both compressive strength and abrasion durability, confirming their suitability for flooring applications. Similarly, Zhou *et al.* (2019) demonstrated that surface densification of poplar (*Populus tomentosa*) improves the density profile and hardness, both of which are directly linked to abrasion resistance. At the microstructural level, Leiter *et al.* (2022) investigated triboelectric surface activation and found that brushing, thermal, and mechanical treatments alter surface energy and sliding behavior, affecting friction and wear interactions.

Despite this progress, few studies have examined the wear behavior of different combinations of normal load and sliding speed for African hardwoods, specifically *Tieghemella heckelii* (makore), *Khaya anthotheca* (mahogany), and *Pericopsis elata* (assamela), which are highly prized in both local and international markets. The objective of this study was to investigate the abrasive wear behavior of these species under two-body abrasive contact perpendicular to the grain. The effects of normal load and sliding speed on the wear coefficient were evaluated under dry conditions. Attention was paid to the evolution of wear volume as a function of sliding distance, to the transition from the running-in phase to steady-state wear, and to the specific response of each wood species to variations in load and sliding speed. The results provide comparative data for evaluating the suitability of these tropical hardwoods for applications involving abrasive mechanical contact and contribute to a broader characterization and utilization of Central African timber resources.

EXPERIMENTAL

Wood Species Selection and Specimen Preparation

In this study, three tropical hardwood species makore (*Tieghemella heckelii*), mahogany (*Khaya anthotheca*), and assamela (*Pericopsis elata*) were selected because of their frequent use in mechanical wear applications such as flooring and industrial components. To begin with, rectangular planks were cut from the trunk of each wood species with their longitudinal axis oriented parallel to the grain direction according to the French Standard (NF B51-002).

From these planks, specimens measuring 20 * 20 * 20 mm^3 (R, T, L) were prepared in the radial, tangential, and longitudinal directions, respectively, for the determination of density and for monitoring moisture content during the experimental campaign. In addition, specimens measuring 20 * 20 * 360 mm^3 (R, T, L) were prepared for the determination of the modulus of rupture (MOR) and modulus of elasticity (MOE).

For the tribological tests, circular specimens with a diameter of 112 mm and a thickness of 7 mm were machined with their thickness oriented along the longitudinal direction of the wood. Consequently, the abrasive action occurred perpendicularly to the grain direction (Fig. 1c). This configuration was selected because it simulates practical situations in which wood surfaces are exposed to abrasive wear normal to the fiber direction, such as flooring, furniture surfaces, and structural elements subjected to repeated contact.

All specimens were calibrated and conditioned in the Laboratory of Mechanics and Materials Physics Systems (U2MSP), University of Dschang, under controlled environmental conditions (25 ± 2 °C and 65 ± 5% relative humidity) for eight weeks. During this period, the specimens underwent natural drying and reached hygroscopic equilibrium before testing. The equilibrium moisture content was monitored using the 20 * 20 * 20 mm^3 specimens and was found and recorded in table 1. The basic characteristics of the studied species are recorded in Table 1.



Fig. 1. (a) Wear test device, (b) balance, and (c) worn and unworn specimens

Table 1. Physical and Mechanical Properties of Species

Species	MOR in Static Bending (MPa)		MOE in Static Bending (MPa)		Density (kg/m^3)	
	Value	Humidity	Value	Humidity	Value	Humidity
Makore	46 ± 4	14	9711 ± 3461	14	654 ± 30	14
Assamela	67 ± 7	14	9647 ± 1849	14	669 ± 67	14
Mahogany	46 ± 4	14	7911 ± 493	14	711 ± 26	14

Experimental Setup and Test Conditions

Wear tests were conducted using a Taber abrasimeter (Model DH-TA-01; Guangdong Hongtuo Instrument Technology Co., Ltd., Dongguan, China) (Fig. 1a), equipped with two aluminum oxide abrasive wheels (P120 grit). The abrasive wheels were positioned on opposite sides of the rotating specimen and applied a constant normal load to the wood surface during testing. The experiments were performed under controlled laboratory conditions in dry conditions, using three normal loads: 250, 500, and 750 g. For each wood species, normal load, and rotational speed combination, 10 specimens were tested. Of the 10 specimens prepared for each species, one specimen was selected as representative for each combination of normal load and sliding speed. Thus, the results in this work correspond to one representative specimen for each experimental condition. The remaining specimens were used to verify the consistency of the observed wear trends. For each representative specimen, 25 repetitions of 10 consecutive rotations were performed. The rotational speed of the specimen holder was varied from 20 to 70 rpm in 10 rpm increments, corresponding to a total of six speed levels (20, 30, 40, 50, 60, and 70 rpm). The resulting sliding distance was approximately 4 m per test condition. The same experimental procedure was applied to the three wood species.

Debris Management and Measurement of Mass Loss

To ensure consistent abrasive contact, a suction nozzle was installed directly above the wear track connected to waste vacuum to eliminate wood particles generated during testing. After 10 revolutions, the abrasives wheels were removed and cleaned with a soft brush. For two specimens tested, abrasive wheels were rectified using a sharpening stone. Same, specimens were carefully brushed to remove residual particles and weighed using a MY WEIGH electronic balance with an accuracy of ± 0.01 g (Fig. 1b). The mass loss (Δm) due to wear was then calculated by subtracting the final mass from the initial mass.

Calculation of Worn Volume

The volume of material removed (V) was calculated using the mass loss and the density of each species, as follows,

$$V = {}^{\Delta m}/_{\rho} \quad (1)$$

where Δm is the mass loss (g) and ρ is the density of the wood species (g/cm³).

Calculation of the Wear Coefficient

To evaluate the wear behavior under varying operational conditions, the wear coefficient (k) was determined based on Archard's wear law,

$$k = {}^{V}/_{F.D} \quad (2)$$

where V is the wear volume (mm³), F is the applied normal load (N), and D is the sliding distance (m).

However, to improve accuracy and account for the transitional and steady-state wear behavior, the wear coefficient was computed from the slope of the linear portion of the wear volume *versus* sliding distance curve, corresponding to the steady-state regime. In this regime, the wear mechanism is stabilized, and the volume loss progresses linearly with distance. The identification of the steady-state region was completed by plotting the cumulative wear volume over increasing sliding distance and selecting the portion where a linear trend with minimal fluctuation was observed.

RESULTS AND DISCUSSION

For clarity, the results presented in this study correspond to the representative specimens selected for each experimental condition.

Behavior Depending on the Wear Distance Traveled

The results obtained for the evolution of wear volume as a function of rolling distance (Fig. 2) show two clearly distinct wear regimes: an initial running-in period, lasting approximately 0.138 m, followed by a steady-state wear region. This two stages behavior was consistently observed in the eighteen specimens tested for each wood species, although the curves presented in Fig. 2 correspond to representative specimens selected to illustrate the general behavior. This behavior aligns closely with classical tribological observations across a range of materials, including metals, polymers, and hard coatings (Okokpujie *et al.* 2024).

During the running-in phase, the rapid increase in wear volume may be associated with the progressive adaptation of the wood surface to the abrasive contact. The removal or deformation of surface asperities, together with local fracture and detachment of weakly supported material, may contribute to this initial increase in material loss (Sakhamuri 2023). However, these mechanisms are considered as possible explanations. Similar phenomena have been reported for steels, where the wear rate and friction coefficient increase sharply during the running-in, and then plateau once the surface has adapted (Zambrano *et al.* 2024).

The transition observed at approximately 0.138 m may indicate that the initial adaptation of the wood surface to the abrasive wheels becomes progressively stabilized beyond this distance. The subsequent near linear increase in wear volume suggests that a relatively stable wear regime was established after the running-in stage. This behavior provides a practical basis for determining the steady-state wear coefficient from the slope of the wear volume and sliding distance relationship in accordance to Archard's wear model. The suitability of the steady state linear region is further supported by the regression coefficients (R^2) obtained from the linear trend curves (Fig. 2). For makore and mahogany, R^2 values increased with increasing normal load, indicating an increasingly linear relationship between wear volume and sliding distance. In contrast, R^2 values for Assamela remained relatively stable across the investigated load levels.

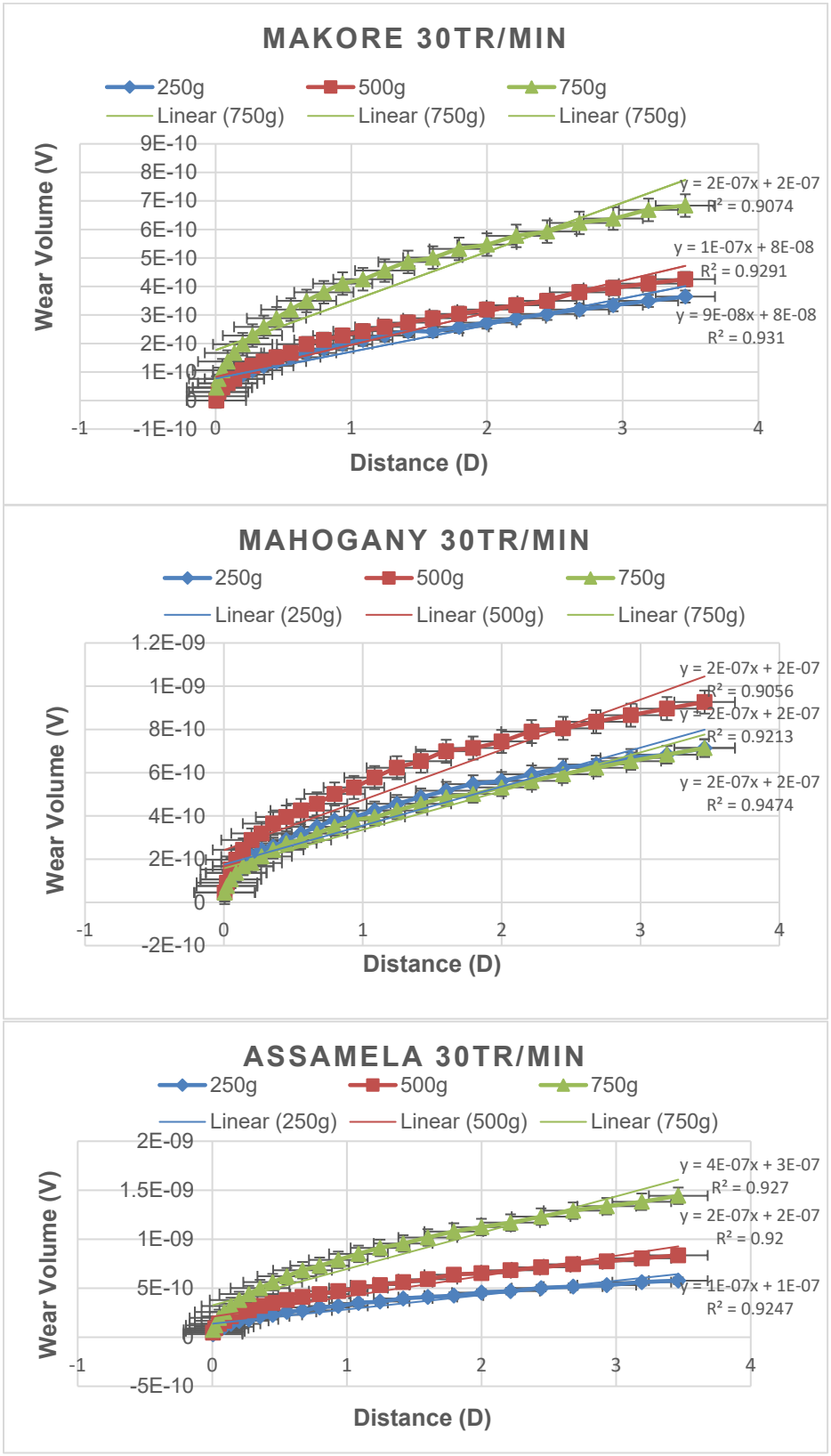


Fig. 2. Representative variation of wear volume as a function of sliding distance for makore, mahogany, and assamela at a rotational speed of 30 rpm under three normal loads (250, 500, and 750 g). The two stages wear behavior shown were consistently observed across the 18 specimens tested for each wood species.

These results support the use of the steady state-region for estimating the wear coefficient under the investigated condition. Importantly, this two-stage behavior was consistent across all tested speeds (20 to 70 rpm), indicating that while sliding speed and load likely affect the magnitude of wear, they do not alter the fundamental wear mechanism. This mirrors findings in polymer-metal systems, where regardless of speed, materials exhibit this bifurcation of wear regimes (Abdelbary 2021).

Wear in Stationary State and Wear Coefficient

To evaluate the wear behavior of the three wood species under different loading and speed conditions, the wear coefficient was calculated using the slope of the linear portion of the wear volume *versus* sliding distance curve (Fig. 2), corresponding to the steady state wear region. In that regime, the wear rate became constant, and the wear mechanism stabilized, making the calculation of the wear coefficient (k) physically meaningful because the variation of the wear volume as a function of the sliding distance at different load revealed that all three wood species generally followed the linear trend predicted by Archard's wear law across all test sliding speeds. This suggests that the increase in wear was, to a first approximation, directly proportional to the sliding distance (Zhai *et al.* 2021).

Influence of Normal Load on Wear Coefficient

As shown in Fig. 3, the experimental results revealed a systematic decrease in the wear coefficient as the applied normal load increased from 250 to 750 g across the investigated sliding speeds. This trend indicates that the wear coefficient was not independent of the applied load over the investigated range. Although Archard's relationship predicts a proportional increase in wear volume with increasing normal load under idealized conditions, the wear coefficient may vary when the contact conditions and deformation response of the material change with load.

The present results suggest that the tribological response of the investigated woods were load dependent, potentially as a result of changes in the real contact area, local contact pressure, and surface deformation. A particularly marked decrease in the wear coefficient was observed between 250 and 500 g, while the reduction between 500 and 750 g was comparatively smaller. Quantitatively, the wear coefficient decreased by 32.9%, 36.3%, and 34.4% for assamela, makore, and mahogany, respectively, when the load was increased from 250 to 500 g. In contrast, the corresponding decreases between 500 and 750 g were only 10.1%, 13.6%, and 17.5%, respectively. This difference indicates a nonlinear response of the wear coefficient to normal load and suggests a gradual stabilization of the wear response beyond 500 g.

One possible explanation for this behavior is the progressive deformation and compaction of the superficial cellular structure of the wood under increasing normal load. Such deformation could increase the effective area involved in contact and modify the distribution of pressure among the abrasive grains. As the real contact area increases, the local pressure acting on individual abrasive grains may decrease, potentially reducing their penetration into the wood surface and consequently limiting material removal. However, because no direct measurements of real contact area, subsurface deformation, or cellular compaction were performed in the present study, this interpretation should be regarded as a possible mechanism.

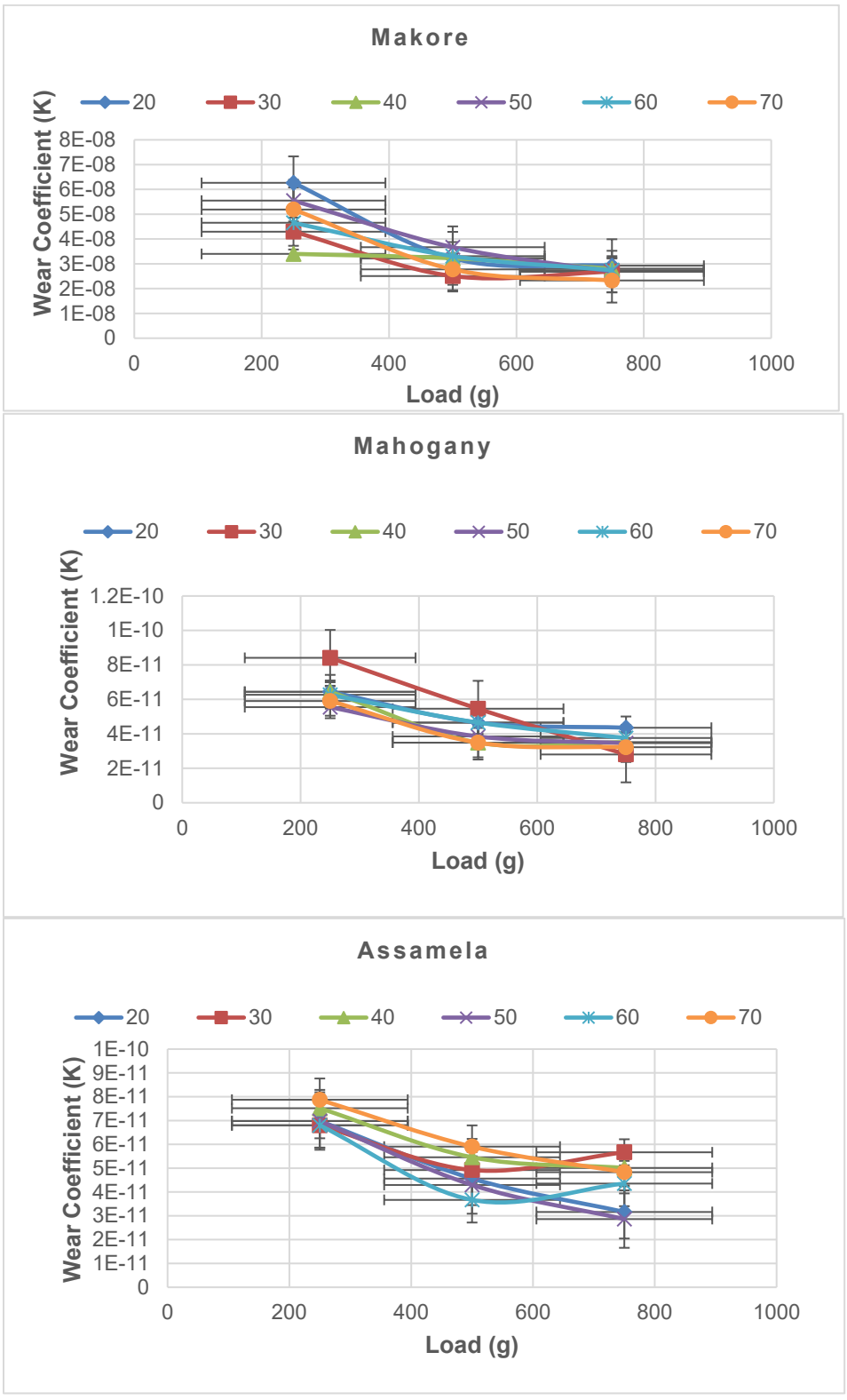


Fig. 3. Evolution of the wear coefficient as a function of applied load for makore, mahogany, and assamela, evaluated across multiple rotational speeds (20 to 70 rpm)

The possibility of progressive surface smoothing or self-polishing should also be considered cautiously. Repeated abrasive interactions may remove loosely attached

material and modify the surface topography, potentially leading to a more stable contact condition at higher loads. However, since surface roughness and wear-track morphology were not measured, the occurrence of a self-polishing mechanism cannot be directly confirmed from the present data. Overall, the results indicate that increasing the normal load from 250 to 750 g reduced the wear coefficient for all three investigated species, with the most pronounced reduction occurring between 250 and 500 g. Above 500 g, the magnitude of the reduction became smaller, suggesting a progressive stabilization of the wear response. This load-dependent behavior indicates that the wear coefficient is influenced by changes in the abrasive contact conditions.

Influence of Wear Rate on Wear Coefficient

The variation of the wear coefficient as a function of speed, for each applied load, revealed a non-monotonic trend across the three investigated wood species (Fig. 4). In contrast to the linear response typically expected from Archard's law under stable contact conditions, the wear coefficient exhibited both minima and maxima at specific speed intervals. This pattern was consistent across all load levels.

Such irregular variations indicate that wear behavior in wood is governed by complex tribological phenomena, involving mechanism transitions as sliding speed changes. The observed stabilisation of the wear response may be associated with changes in the worn surface during sliding. Although the formation of tribofilm cannot be confirmed, despite the fact similar behaviors has been observed in aluminum alloys where tribo-films formed adaptively under variable surface interactions, reducing wear during sliding (Silva *et al.* 2023), in addition to that hypothesis, the possibility of progressive smoothing surface cannot be excluded. However, the speed dependent variation in wear coefficient may partly be related to frictional heating, since interface temperature was not measured, thermal degradation can't be confirmed from the present experiments.

A broader perspective on non-monotonic behavior is provided by Brink *et al.* (2020), who developed a parameter-free model for adhesive wear, showing that particle detachment rates vary nonlinearly with sliding conditions due to evolving contact mechanics and detachment thresholds. These findings support the hypothesis that speed not only changes the contact smoothing and temperature at the interface but also triggers shifts in the dominant wear mechanisms, debris removal efficiency, and tribofilm formation, all crucial factors in wood tribology. Finally, analogous behavior was observed by Zhang *et al.* (2022) in degradation of polymer composites under sliding: an optimal speed window minimizes wear, while both lower and higher speeds lead to increased wear due to shifts between abrasive and fatigue mechanisms.

This implies that there exists an optimal speed range for each wood species, at which the wear coefficient reaches a minimum. Identifying these thresholds can inform the design of wood components exposed to frictional loading to maximize wear resistance under practical use conditions.

Comparative and Statistical Analysis of the Effect of load and Speed on Wear Behavior across Species

The influence of sliding speed on the abrasive wear behavior of *Tieghemella heckelii* (makore), *Khaya anthotheca* (mahogany), and *Pericopsis elata* (assamela) was investigated at three normal loads of 250, 500, and 750 g. The corresponding results are summarized in Table 2. Unlike the systematic decrease observed with increasing normal load, the wear coefficient exhibited a non-monotonic dependence on sliding speed. The

speed associated with the minimum or maximum wear coefficient varied according to both wood species and applied load, indicating that the effect of sliding speed was species and load dependent.

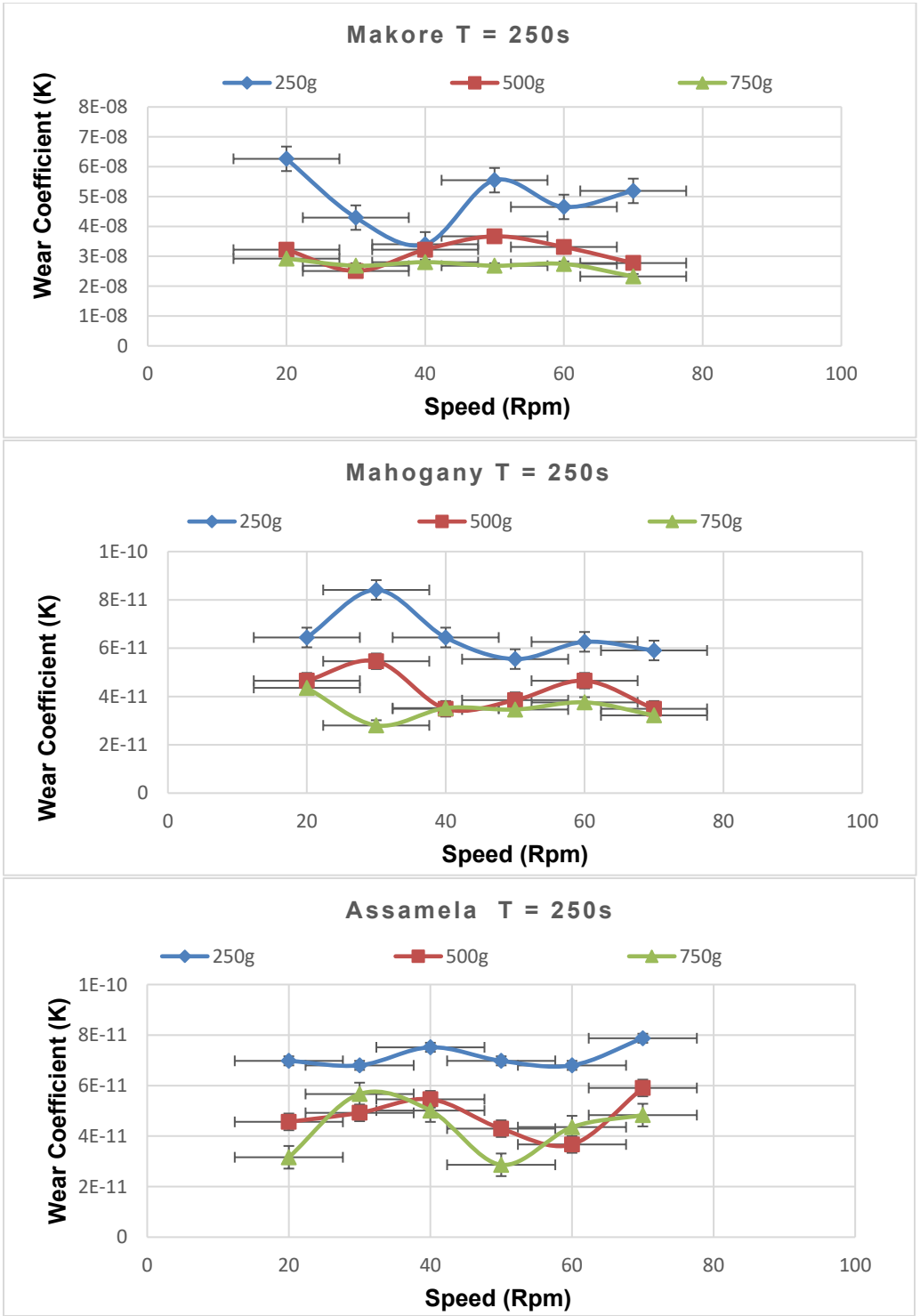


Fig. 4. Variation of the wear coefficient as a function of sliding speed for makore, mahogany, and assamela at different applied load levels (250, 500, and 750 g)

Table 2. Minimum, Mean, and Maximum Wear Coefficients and their Corresponding Sliding Speeds for Makore, Mahogany, and Assamela at Different Normal Loads

		Wear Coefficient ($10^{-8}.{mm^3}/{N.m}$) and Corresponding Speed (rpm)		
Species	Load	Minimal	Mean	Maximal
Makore	250 g	(40 ; 3.40)	(60 ; 4.65)	(20 ; 6.26)
	500 g	(30 ; 2.50)	(40 ; 3.22)	(50 ; 3.66)
	750 g	(70 ; 2.32)	(30 ; 2.68) ; (50 ; 2.68)	(20 ; 2.92)
Mahogany	250 g	(50 ; 5.54)	(20 ; 6.44) ; (40 ; 6.44)	(30 ; 8.41)
	500 g	(40 ; 3.48)	(20 ; 4.65) ; (60 ; 4.65)	(30 ; 5.45)
	750 g	(30 ; 2.80)	(40 ; 3.51)	(20 ; 4.35)
Assamela	250 g	(30 ; 6.80) ; (60 ; 6.80)	(20 ; 6.97)	(70 ; 7.87)
	500 g	(60 ; 3.66)	(30 ; 4.92)	(70 ; 5.90)
	750 g	(50 ; 2.86)	(60 ; 4.35)	(30 ; 5.66)

For makore at 250 g, the wear coefficient decreased from $6.26*10^{-8}\,{mm^3}/{N.m}$ at 20 rpm to a minimum of $3.40*10^{-8}\,{mm^3}/{N.m}$ at 40 rpm followed by an increase to $4.65*10^{-8}\,{mm^3}/{N.m}$ at 60 rpm. A similar non monotonic response was observed at 500 g, although the minimum occurred at 30 rpm. At 750g, the minimum wear coefficient was obtained at the highest investigate speed, 70 rpm with a value of $2.32*10^{-8}\,{mm^3}/{N.m}$. Mahogany also exhibited a non-monotonic response. At 250 g, the wear coefficient reached a maximum of $8.41*10^{-8}\,{mm^3}/{N.m}$ at 30 rpm and a minimum of $5.54*10^{-8}\,{mm^3}/{N.m}$ at 50 rpm. At 500 g, the maximum value was observed at 30 rpm, whereas the minimum occurred at 40 rpm. At 750g, the wear coefficient decreased to $2.80*10^{-8}\,{mm^3}/{N.m}$ at 30 rpm and increased to $4.35*10^{-8}\,{mm^3}/{N.m}$ at 20 rpm. Assamela showed a similarly complex response. At 500 g, the minimum wear coefficient was obtained at 60 rpm, whereas the maximum occurred at 70 rpm. At 750 g, the minimum was observed at 50 rpm, while the maximum occurred at 30 rpm.

The occurrence of speed-dependent minima and maxima indicates that the relationship between sliding speed and abrasive wear coefficient can't adequately represented by a linear trend over the investigate range.

Figure 5 shows the variation in the average wear coefficient as a function of the applied normal load for assamela, makore, and mahogany. A similar decreasing trend in the average wear coefficient was observed for all three wood species as the applied load increased from 250 to 750 g. However, the magnitude of this reduction differed among the species. Makore consistently exhibited the lowest average wear coefficient at all investigated load levels, whereas assamela showed the highest values. Thus, the ranking of the species remained unchanged over the investigated load range, with

$$k_{Makore} < k_{Mahogany} < k_{Assamela}$$

at 250 g, 500 g, and 750 g. This result indicates that, based on the average wear coefficient, makore exhibited the highest abrasive wear resistance among the three investigated species, whereas assamela exhibited the lowest resistance under the experimental conditions considered. However, these differences should be interpreted in conjunction

with the statistical significance of the observed variations. The effect of normal load on the wear response of wood is consistent with the complex tribological behavior expected from an anisotropic and heterogeneous biological material. Unlike homogeneous engineering materials, wood has a hierarchical cellular structure whose mechanical and tribological response depends on its anatomical characteristics, density, moisture content, and fiber orientation. Recent studies have emphasized that wood's tribological behavior is strongly influenced by its physical structure and processing conditions, with anisotropy and the porous cellular architecture playing important roles in friction and wear behavior Dong *et al.* (2022). The numerical values presented in Table 3 further quantify the effect of normal load on the wear coefficient.

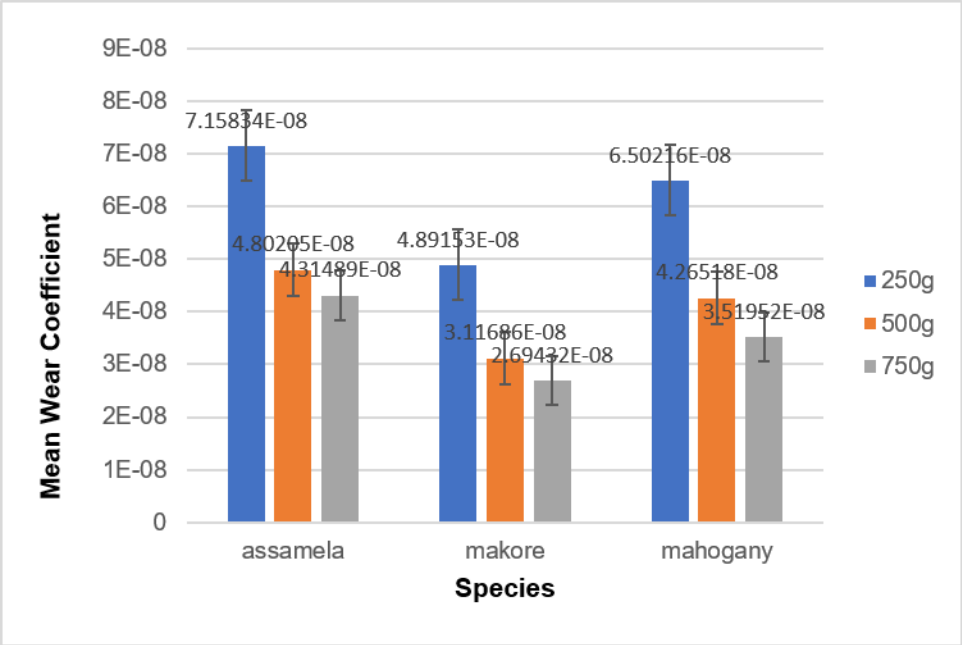


Fig. 5. Variation in the average wear coefficient as a function of the applied load and wood species across the investigated speeds

Table 3. Average Wear Coefficients of Assamela, Makore, and Mahogany Evaluated over Six Sliding-speed Levels (20, 30, 40, 50, 60, and 70 rpm) at Normal Loads of 250, 500, and 750 g

Load/Species	Assamela	Makore	Mahogany
250 g	$7.1583*10^{-8}\ mm^3/_{N.m}$	$4.89153*10^{-8}\ mm^3/_{N.m}$	$6.50216*10^{-8}\ mm^3/_{N.m}$
500 g	$4.8021*10^{-8}\ mm^3/_{N.m}$	$3.11686*10^{-8}\ mm^3/_{N.m}$	$4.26518*10^{-8}\ mm^3/_{N.m}$
750 g	$4.3149*10^{-8}\ mm^3/_{N.m}$	$2.69432*10^{-8}\ mm^3/_{N.m}$	$3.51952*10^{-8}\ mm^3/_{N.m}$

The data in Table 3 indicate that the reduction in the average wear coefficient was more pronounced when the load increased from 250 to 500 g than when it increased from 500 to 750 g. Between 250g and 500g, the average wear coefficient decreased by approximately 32.9% for assamela, 36.3% for makore, and 34.4% for mahogany. In comparison, increasing the load from 500 to 750 g resulted in smaller reductions of

approximately 10.1%, 13.6%, and 17.5% for assamela, makore, and mahogany, respectively.

Therefore, the response of the wear coefficient to increasing normal load was not proportional over the investigated load range. Instead, the results indicate a nonlinear decrease characterized by a pronounced reduction between 250 and 500 g followed by a weaker reduction between 500 and 750 g. The latter observation suggests that the wear response tends to become less sensitive to further increases in load above 500 g.

A possible explanation for the reduction in the apparent wear coefficient is therefore that increasing load modifies the real contact area and the local deformation state of the wood surface. Progressive deformation or compaction of the cellular structure may contribute to this behavior. Recent tribological investigations of compressed wood have demonstrated that changes in wood density and cellular structure can significantly influence its friction and wear behavior, supporting the possibility that structural deformation may contribute to the observed response (Waßmann and Ahmed 2024). Besides, because wood is a porous and mechanically heterogeneous material, these changes may alter the relative contributions of micro-cutting, micro-ploughing, localized deformation, and cell-wall fracture during abrasive contact. Abrasive wear in wood-processing applications is generally associated with mechanisms such as micro-cutting, micro-ploughing, and microcracking, whose relative contributions depend on the characteristics of both the wood and the contacting abrasive surface (Muhammed *et al.* (2023).

The observed decrease in the wear coefficient suggests that the proportionality between wear volume and applied load is not sufficient to describe the complete tribological response of these wood species over the investigated load range. Changes in real contact area, local pressure distribution, deformation behavior, and surface morphology may cause the apparent wear coefficient to vary with load.

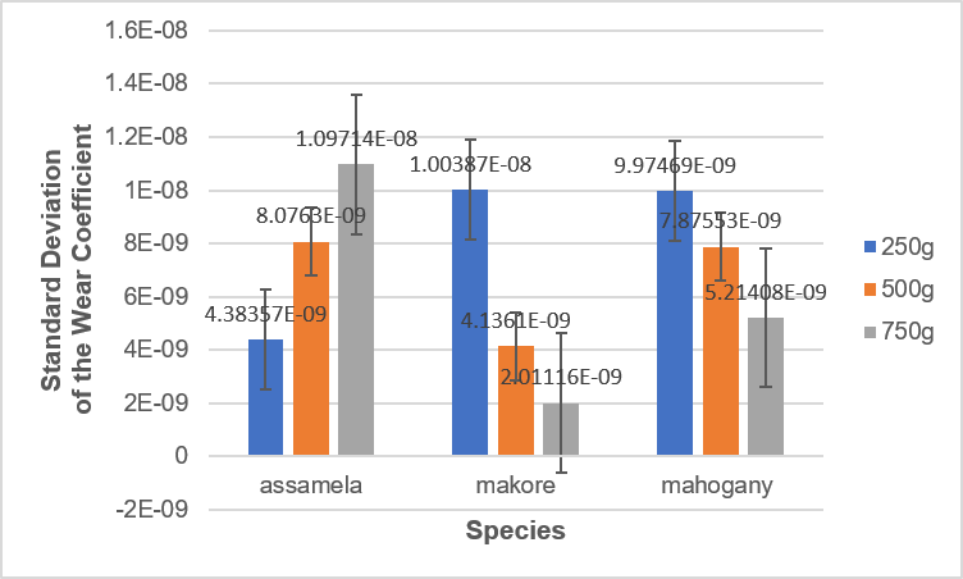


Fig. 6. Variation in the standard deviation of the wear coefficient as a function of applied load and wood species across the investigated speeds

Figure 6 presents the standard deviation of the wear coefficient calculated from the six investigated sliding-speed levels for each wood species and normal load. The three

species exhibited distinct trends in the dispersion of the wear coefficient. For assamela, the standard deviation increased progressively with increasing normal load. In contrast, makore and mahogany exhibited decreasing standard deviations as the load increased, with the reduction being considerably more pronounced for makore.

Table 4. Standard Deviations of the Wear Coefficients of Assamela, Makore, and Mahogany Calculated from Six Sliding-speed Levels (20, 30, 40, 50, 60, and 70 rpm) at Normal Loads of 250, 500, and 750 g

Load/Species	Assamela	Makore	Mahogany
250g	$4.3836*10^{-9}\ \boldsymbol{mm^3}/_{\boldsymbol{N.m}}$	$1.0039*10^{-8}\ \boldsymbol{mm^3}/_{\boldsymbol{N.m}}$	$9.9747*10^{-9}\ \boldsymbol{mm^3}/_{\boldsymbol{N.m}}$
500g	$8.0763*10^{-9}\ \boldsymbol{mm^3}/_{\boldsymbol{N.m}}$	$4.1361*10^{-9}\ \boldsymbol{mm^3}/_{\boldsymbol{N.m}}$	$7.8755*10^{-9}\ \boldsymbol{mm^3}/_{\boldsymbol{N.m}}$
750g	$1.0971*10^{-8}\ \boldsymbol{mm^3}/_{\boldsymbol{N.m}}$	$2.0112*10^{-9}\ \boldsymbol{mm^3}/_{\boldsymbol{N.m}}$	$5.2141*10^{-9}\ \boldsymbol{mm^3}/_{\boldsymbol{N.m}}$

As shown in Table 4, the standard deviation for assamela increased from $4.3836*10^{-9}\ mm^3/_{N.m}$ at 250g to $1.0971*10^{-8}\ mm^3/_{N.m}$ at 750g, corresponding to an increase of approximately 150%. Conversely, makore exhibited a marked reduction in standard deviation, from $1.0039*10^{-8}\ mm^3/_{N.m}$ to $2.0112*10^{-9}\ mm^3/_{N.m}$, corresponding to an approximately 80% decrease. Mahogany showed an intermediate behavior, with the standard deviation decreasing by approximately 48% between 250 and 750 g.

These results indicate that the effect of normal load on the dispersion of the wear coefficient was species-dependent. The simultaneous decrease in the average wear coefficient and standard deviation observed for makore suggests that this species exhibited not only a lower mean wear response but also a progressively narrower distribution of wear coefficient values over the investigated speed levels as the load increased. Mahogany showed a similar, although less pronounced, tendency. In contrast, the increase in standard deviation observed for assamela indicates that the wear coefficient became more dispersed across the investigated speed levels at higher loads. It is important to note that the standard deviations reported here describe the dispersion of the six wear-coefficient values associated with the six investigated sliding speeds. Therefore, they should not be interpreted directly as a measure of experimental reproducibility or repeatability. Rather, they indicate the extent to which the wear coefficient varied across the investigated speed conditions at a given load.

The contrasting evolution of the standard deviation among the species may reflect differences in the way their heterogeneous anatomical structures respond to changes in load and sliding speed. The progressive reduction in dispersion observed for makore and mahogany may indicate a more uniform wear response under the higher load conditions investigated. Such a hypothesis is compatible with the known sensitivity of wood tribological behavior to density, cellular structure, surface condition, and loading conditions. However, the present experimental data do not allow a direct attribution of this behavior to a specific microstructural mechanism. For assamela, the increase in standard deviation with load may indicate a greater sensitivity of its wear response to the changes in sliding conditions imposed by the higher normal loads. However, this interpretation should also be regarded as a hypothesis because the present study did not directly characterize the anatomical or surface changes occurring during abrasion.

Overall, the combined analysis of the average wear coefficient and its standard deviation shows that increasing the normal load reduced the mean wear coefficient for all

three wood species, while its effect on the dispersion of the wear response depended on the species. Makore exhibited the lowest average wear coefficient throughout the investigated load range and simultaneously showed a substantial reduction in dispersion with increasing load. These characteristics suggest that makore provided the most favorable abrasive-wear response among the three species under the tested conditions.

CONCLUSIONS

This study examined the abrasive wear behavior of *Tieghemella heckelii* (makoré), *Khaya anthotheca* (mahogany), and *Pericopsis elata* (assamela) under various normal loads and at different sliding speeds. The effects of normal load and sliding speed on the wear coefficient were studied under dry, unlubricated conditions. In addition, the quantitative results presented for each experimental condition were obtained from representative samples, while other samples were used to verify the consistency of the observed qualitative trends.

1. All three wood species exhibited two-phase wear behavior, consisting of an initial running-in phase followed by a quasi-linear steady-state regime. The transition occurred at a sliding distance of approximately 0.138m. This behavior was consistently observed across all tested samples. The steady-state region provided a suitable basis for determining the wear coefficient from the slope of the relationship between the wear volume and the sliding distance.
2. The results indicated a nonlinear dependence on load and suggested a gradual stabilization of the wear response beyond 500 g. The decrease was particularly pronounced between 250 and 500 g, reaching approximately 32.9% for assamela, 36.3% for makore, and 34.4% for mahogany. Between 500 and 750 g, the corresponding decreases were less significant, amounting to approximately 10.1%, 13.6%, and 17.5%, respectively. This behavior does not contradict Archard's relationship but rather indicates that the wear coefficient is not constant when the contact and deformation conditions at the wood-abrasive interface vary with load.
3. Clear differences were also observed among the three wood species. Based on the average wear coefficient, makore exhibited the highest resistance to abrasive wear under the conditions studied, followed by mahogany and assamela at all load levels.
4. It was observed that an increase in sliding speed did not result in a simply proportional increase or decrease in abrasive wear, and that there may be critical speed ranges for each wood species and each load level. This behavior underscores the importance of considering the interaction between normal load and sliding speed when evaluating the suitability of tropical hardwoods for applications involving abrasive contact.
5. Analysis of the dispersion of the wear coefficient also revealed species-specific responses to increasing load. Makore exhibited a significant decrease in dispersion, indicating a more uniform response to higher loads, while mahogany showed a moderate decrease. Conversely, assamela exhibited an increase in dispersion as the load increased. These differences suggest that the load influences not only the extent of abrasive wear but also the consistency of the tribological response.

From a technical standpoint, the results showed that the abrasion behavior of tropical hardwoods depended on the operating conditions. The relatively low wear coefficients observed for makore, particularly under high loads, indicate that it may be suitable for applications requiring resistance to abrasive surface degradation. More generally, the load and speed-dependent behavior demonstrated experimentally provides useful information for the selection and design of wood materials subjected to abrasive contact. These results demonstrate that the abrasion wear behavior of tropical hardwoods depends strongly on both the wood species and the operating conditions. The proposed mechanisms, involving surface deformation and contact stabilization, remain hypotheses and will need to be verified through microscopic analyses and surface characterization in future studies.

ACKNOWLEDGEMENTS

During the preparation of this work, the authors used Chat GPT AI to translate language from French to English and correct grammatical errors. Additionally, the tool was used to rephrase certain sentences to ensure they were easily understandable and clear for the readers. Authors reviewed and edited the content as needed and take full responsibility for the final content of the published article.

REFERENCES CITED

Abdelbary, A. (2021). "Friction and wear of polymer and polymer composites," in: *Tribology of Polymer and Polymer Composites for Industry 4.0*, Springer Singapore, Singapore, pp. 33-54. https://doi.org/10.1007/978-981-16-3903-6_3

Brink, T., Frérot, L., and Molinari, J.-F. (2020). "A parameter-free mechanistic model of the adhesive wear process of rough surfaces in sliding contact," *Journal of the Mechanics and Physics of Solids* 145, article 104238. https://doi.org/10.1016/j.jmps.2020.104238

Dong, C., Yang, Y., Yuan, C., Bai, X., and Guo, Z. (2022). "Effects of anisotropy of lignum vitae wood on its tribological performances," *Composites Part B: Engineering* 228, article 109426. https://doi.org/10.1016/j.compositesb.2021.109426

Gendvilas, V., Downes, G. M., Lausberg, M., Harrington, J. J., and Lee, D. J. (2024). "Predicting wood density using resistance drilling: The effect of varying feed speed and RPM," *Forests* 15(4), article 579. https://doi.org/10.3390/f15040579

Ghadiri, M., Azdast, T., and Heravi, G. (2021). "Effect of tool wear and cutting parameters on wear mechanisms in machining laminated wood composites," *Wear* 476, article 203521. https://doi.org/10.1016/j.wear.2020.203521

Guan, H., Zhang, J., Li, X., and Lyu, J. (2024). "Tribological properties of densified wood under different sliding conditions," *Tribology International* 191, article 109156. https://doi.org/10.1016/j.triboint.2023.109156

Leiter, L. M., Myna, R., Frömel-Frybort, S., Liebner, F., and Wimmer, R. (2022). "Triboelectric surface field strength of wood after brushing," *Wood Science and Technology* 56(6), 1401-1417. https://doi.org/10.1007/s00226-022-01411-z

Muhammed, M., Javidani, M., Heidari, M., and Jahazi, M. (2023). "Enhancing the tribological performance of tool steels for wood-processing applications: A

comprehensive review," *Metals* 13(8), article 1460. https://doi.org/10.3390/met13081460

Nasir, V., and Cool, J. (2018). "A review on wood machining: Characterization, optimization, and monitoring of the sawing process," *Wood Material Science & Engineering* 15(3), 1-16. https://doi.org/10.1080/17480272.2018.1465465

Okokpujie, I. P., Tartibu, L. K., Musa-Basheer, H. O., and Adeoye, A. O. M. (2024). "Effect of coatings on mechanical, corrosion and tribological properties of industrial materials: A comprehensive review," *Journal of Bio-and Tribo-Corrosion* 10(1), article 2. https://doi.org/10.1007/s40735-023-00805-1

Sakhamuri, M. S. D., Harvey, T. J., Vierneusel, B., and Wood, R. J. (2023). "Wear induced changes in surface topography during running-in of rolling-sliding contacts," *Wear* 522, article 204685. https://doi.org/10.1016/j.wear.2023.204685

Silva, R. D., Martins, P. A., and Santos, M. (2023). "Tribofilm formation and wear reduction in dry sliding of aluminum alloys," *Advanced Engineering Materials* 180, article e14002. https://doi.org/10.1002/adem.202400142

Snow, D., Khademibami, L., Sherrington, A., Shmulsky, R., Montague, I., Ross, R. J., and Wang, X. (2022). "Effect of thermomechanical densification treatment on abrasion resistance of five US hardwoods," *Forest Products Journal* 72(3), 175-179. https://doi.org/10.13073/FPJ-D-22-00028

Tenorio, C., and Moya, R. (2020). "Effect of thermo-hydro-mechanical densification on the wood properties of three short-rotation forest species in Costa Rica," *BioResources* 15(4), 8065-8084. https://doi.org/10.15376/biores.15.4.8065-8084

Torkghashghaei, M., Shaffer, W., Ugulino, B., Georges, R., Hernández, R. E., and Blais, C. (2022). "Improvement of the wear resistance of circular saws used in the first transformation of wood through the utilization of variable engineered micro-geometry performed on PVD-coated WC-Co tips," *Applied Sciences* 12(23), article 12213. https://doi.org/10.3390/app122312213

Waßmann, O., and Ahmed, S. U. (2024). "Tribological properties and related effects of compressed, thermally modified and wax-impregnated wood," *European Journal of Wood and Wood Products* 82(6), 2155-2168. https://doi.org/10.1007/s00107-024-02145-4

Zambrano, O. A., Iglesias-Guerrero, B., Rodríguez, S. A., and Coronado, J. J. (2024). "Running-in period during sliding wear of austenitic steels," *Tribology Letters* 72(3), 70. https://doi.org/10.1007/s11249-024-01867-z

Zhai, W., Bai, L., Zhou, R., Fan, X., Kang, G., Liu, Y., and Zhou, K. (2021). "Recent progress on wear-resistant materials: designs, properties, and applications," *Advanced Science* 8(11), article 2003739. https://doi.org/10.1002/advs.202003739

Zhang, X., Liu, Y., Wang, J., and Huang, R. (2022). "Non-monotonic wear response in polymer composites under varying sliding speeds: Optimal speed regimes and mechanism transitions," *Materials* 17(2), article 281. https://doi.org/10.3390/ma17020281

Zhou, Q., Chen, C., Tu, D., Zhu, Z., and Li, K. (2019). "Surface densification of poplar solid wood: Effects of the process parameters on the density profile and hardness," *BioResources* 14(2), 4814-4831. https://doi.org/10.15376/biores.14.2.4814-4831

Article submitted: August 11, 2025; Peer review completed: July 11, 2026; Revised version received and accepted: August 31, 2026; Published: September 30, 2026.
DOI: 10.15376/biores.21.4.11211-11227